

PARTICLE AND ACCELERATOR PHYSICS AT THE VEPP-4M COLLIDER

V. Kiselev for the VEPP-4 team [1]
 BINP, Novosibirsk 630090, Russia

Abstract

VEPP-4M electron-positron collider is now operating with KEDR detector for high-energy physics experiments in the 1.5–4.0 GeV beam energy range to study production of hadrons in continuum and for precise measurement of R constant. In parallel with these experiments, the VEPP-4M scientific team carries out a number of accelerator physics investigations. Here are some of them: stabilization of the guide field of VEPP-4M with an accuracy of 10^{-6} using a special feedback system, development of the method of RF orbit separation of electron and positron beams at VEPP-4M instead of usual electrostatic orbit separation for CPT-theorem testing experiment, finding ways to increase luminosity of VEPP-4M. The paper discusses the recent results, present status and prospective plans for the facility.

nuclear physics experiments is operating at VEPP-3. Some physical technical characteristics of the complex make it possible to design experiments that are unique not only for Russia but for the world as a whole.

INTRODUCTION

The VEPP-4M is the modernized VEPP-4 collider, which was commissioned for the first time in 1977. At present, the complex [2] includes (Fig. 1) a Positron injector, VEPP-3 booster accumulator with beam energy in the range from 350 MeV to 2 GeV, VEPP-4M electron-positron collider with beam energy E in the range from 0.9 to 5.5 GeV (Table 1), and KEDR universal magnetic detector [3].

Table 1: Main Parameters of VEPP-4M

Parameters	Values	Units
Circumference	366	m
Tunes Q_H/Q_V	8.54/7.58	
Mom. compaction	0.017	
Max. energy	5.5	GeV
Nat. chromaticity C_H/C_V	-13/-20	
RF-frequency	181.8	MHz
Harmonic number	222	
RF power	0.3	MW
RF voltage	5	MV
No. of bunches per beam	2	
Interaction point		
β_V function	0.05	m
β_H function	0.75	m
D_H function	0.80	m

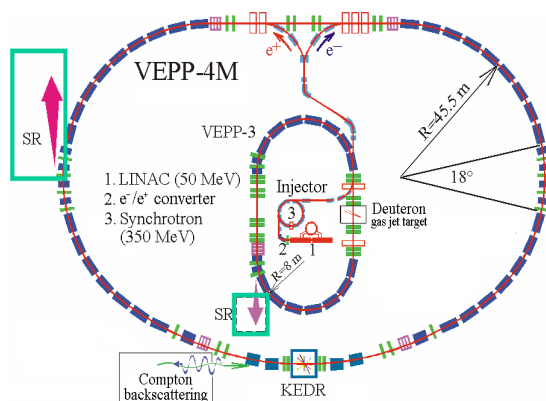


Figure 1. The layout of the VEPP-4 complex.

In addition to the KEDR detector, the experimental spacing of the collider contains a system for registering scattered electrons and positrons for two-photon physics. The VEPP-3 and VEPP-4 facilities are equipped with user stations for studies on the extracted SR beams. A Deuteron unit with the internal polarized gas target for

HIGH-ENERGY PHYSICS

The luminosity of VEPP-4M is a bit lower than the corresponding value in new-generation colliders. For this reason, the KEDR physical program is directed at precision measurements of the parameters of fundamental particles. The following advantages are used in this case: a broad energy range of the center of mass at the complex ($2E = 2-10$ GeV), the methods and techniques that have been developed for the precision determination of the beam energy [4, 5], the fine energy and spatial resolution in a LKr calorimeter (3.5% and 1 mm, $E = 1.8$ GeV), and the high resolution in the system of scattered electrons (10^{-2}). A number of HEP experiments have been carried out at the VEPP-4 complex over the years of its operation since 1980: spectroscopy of the c and b states, including precision measurements of the masses of fundamental particles (the particles from J/ψ , $\psi(2S)$, $\psi(3770)$ and Y families, and D mesons), as well as of the lepton masses and total widths of narrow resonances (Γ_{ee} and Γ_{tot}); measurement of the tau lepton mass proceeding from the threshold behavior of the production cross section (near $E = 1777$ MeV); the unique measurement of fundamental parameter R in the wide energy range of $2E = 2-10$ GeV at one facility; and studies of two-photon physics (full cross section of the $\gamma\gamma \rightarrow$ hadrons process and charge parity states) [6-12].

Here are some recent results:

1) A high-precision determination of the main parameters of the $\psi(2S)$ and $\psi(3770)$ resonances has been performed [13-14]. Fitting the energy dependence of the multihadron cross section in the vicinity of the $\psi(2S)$ has also been carried out (Fig.2, left)

2) The ratio of the electron and muon widths of the J/ψ meson has been measured using direct J/ψ decays (Fig.2, right). The result $\Gamma_{e+e}(J/\psi)/\Gamma_{\mu+\mu}(J/\psi) = 1.0022 \pm 0.0044 \pm 0.0048$ is in a good agreement with the lepton universality [15].

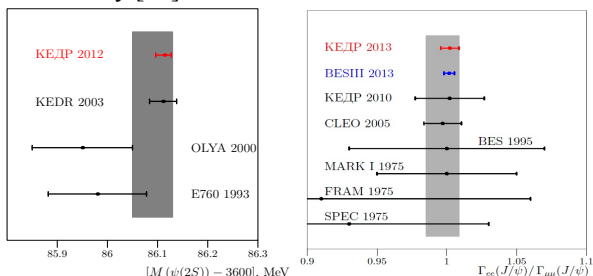


Figure 2. On the left: the compilation of the results on $\psi(2S)$ mass. The relative accuracy of the KEDR result is about $2 \cdot 10^{-6}$. On the right: the measurement result $\Gamma_{e+e}/\Gamma_{\mu+\mu}$.

The following experiments are planned for 2014: scanning at energy $2E = 3.1-4.0$ GeV for the measurement of R and collection of statistical data at the peak of the $\psi(3770)$ meson to measure the mass D_{mesons} .

NUCLEAR PHYSICS

The electro-nuclear experiments with internal targets at the electron-positron storage ring VEPP – 3 have been performed by BINP for several years [16]. During this time the data on the tensor analyzing power in reactions with deuteron have been obtained, the two-photon exchange contribution in (ep) -scattering have been measured.

Further progress of experiments is connected with introduction into VEPP-3 a quasi-real photon tagging system, which will allow performance of a series of measurements of the polarization observables in various reactions with photon energy of up to 1.5 GeV. Creation of the tagging system will be an important stage in development of the technique of experiments with internal targets at the VEPP-3 storage ring. The system will considerably simplify process of event reconstruction of different reactions. Moreover, a significant part of the photons is determined by their transverse polarization that enables to carry out experiments with double polarization.

New experimental section "Deuteron", including the tagging system, differs essentially from the previous one. The new section, in addition to a storage cell, elements of vacuum pumping and quadrupole lenses, comprises three

new dipole magnets and a scattered electron registration system (Fig. 3).

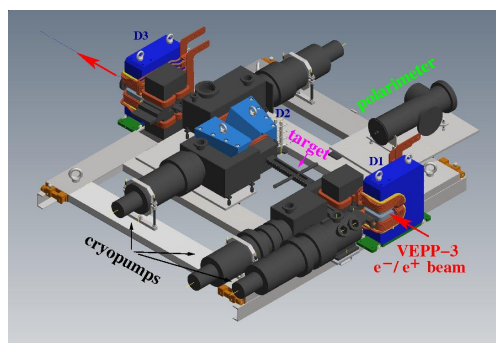


Figure 3. Layout of a new experimental section "Deuteron".

In 2013 the tagging system was introduced into VEPP-3 ring and tested with electron and positron beams. The spectra of the bremsstrahlung and the annihilation radiation were detected at zero angle of the tagging system (Fig.4).

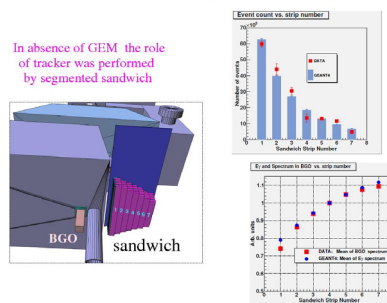


Figure 4. Test of the photon tagging system trigger.

SR EXPERIMENTS

Experiments with synchrotron radiation have been carried out at VEPP-3 for more than 30 years and few years ago at VEPP-4M. Fifteen stations are installed in the experimental halls providing study on X-ray lithography, high pressure and time resolving diffractometry, EXAFS, X-ray fluorescence analysis, X-ray microscopy, small-angle scattering and others.

More than 60 works performed at the VEPP-3 and VEPP-4M storage rings were presented at the XXth National Conference on Synchrotron Radiation "SR - 2014" held recently in Novosibirsk [17]. Installation of a new 7-polar electromagnetic wiggler with a 1.2 T field has provided a increase of radiation intensity by an order of magnitude and reduction of wave length. This has extended possibilities to study the fast processes proceeding in a detonation wave, at the front of a shock wave, and to begin a new program of experiments in diffractometry with a very high time resolution. Thus, for example, the method of acquisition of phase-contrast images with use of X-ray Talbot interferometer, produced

in BINP, has been implemented. Monochromatic radiation with a 0,3 Å wave length was chosen for testing. A fruit of hautbois strawberry (*Fragaria moschata*) with a low absorption contrast at the specified wave length (Fig. 5) was taken as a research subject.

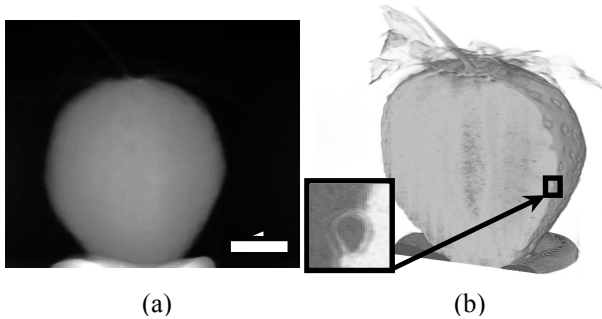


Figure 5. (a) – Absorption contrast, (b) – Tomographically reconstructed three-dimensional structure of a strawberry from a set of phase projections.

Small low-contrast details, such as a stalk, leaves and seeds which are not distinguishable at absorption contrast are well visible. The Talbot interferometer, created at VEPP-4M and used for solving problems of a computer X-ray tomography and microscopy, opens up possibilities for research in such science fields as: geology, materials technology, archeology, biology and are especially important for medical research.

MODERNIZATION OF THE VEPP-4M PICK-UPS

A BINP-developed wideband beam position monitor (BPM) electronics as been installed at the VEPP-4M electron-positron collider [14]. VEPP-4M operates with two electron and two positron bunches. Wide bandwidth of new electronics (210 MHz) allows separation of the measurements of electron and positron bunches with the time interval between the bunches of up to 20 ns. 15 of 54 collider BPMs located near four meeting points are supplied with new electronics. The electronics can measure the position of each of four bunches. BPM system works in two modes: slow closed-orbit measurements and turn-by-turn measurements (Fig.6). With new electronics the accuracy of closed orbit measurements (~3 μm) and turn-by-turn measurements (~15 μm) has increased significantly.

HIGH-FREQUENCY SEPARATION OF ORBITS

At the beginning of 2013, we tested a system for separation of electron and positron orbits in the parasitic collision point that had been recently suggested and developed at the Institute of Nuclear Physics [15]. It is designed to be used instead of traditional electrostatic separation of orbits in the precision experiment on

verifying the CPT invariance by comparison of the electron and positron spin frequencies by the RD method [4].

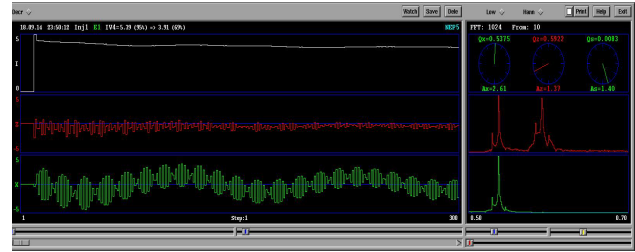


Figure 6. The example of the turn-by-turn measurement of the intensity, vertical (the middle plot) and horizontal (the lower plot) oscillations of the injected beam. The spectra of the oscillations and the calculated deviations of the injection conditions from the optimal values are shown on the right.

In this experiment, the electrostatic method can give a systematic error of about 10^{-6} at the required value of 10^{-9} . The alternative method is based on the application of a high-frequency radial electric field with a frequency strictly equal to half of the circulation frequency of a particle in the collider ($f_0 = 819$ kHz). The plates on which the above-mentioned field is generated are located on the same azimuth with the parasitic collision point. The electron and positron beams in this case circulate on the common orbit, closing after two turns (Fig. 7)

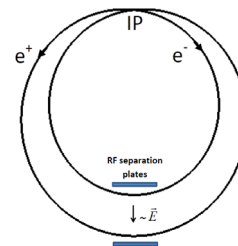


Figure 7. A schematic two-turn orbit in the form of a plane Pascal's snail.

Hence, the systematic error of the CPT experiment connected with the difference in the integrals of a magnetic field along the electron and positron orbits is minimized. The radial bias of the orbit on the high frequency separation azimuth is expressed as follows:

$$X = \frac{\theta\beta}{2 \sin 2\pi\nu_x} (\cos 2\pi\nu_x - 1)$$

where θ is the angle of deflection in the field of the plates and β is the local value of the horizontal β_x function. Near the integer frequency values of the radial betatron oscillations, $\nu_x \rightarrow n$, we have $X \rightarrow 0$. Near the half-integer values, $\nu_x = (2n + 1)/2 + \epsilon$, the X bias becomes significant ($\epsilon \ll 1$): $X \approx \theta\beta/(2\pi\epsilon)$. According to the performed numerical simulation of the collision effects, it

is necessary to separate the orbits, $2X \geq 7\sigma_x$ (σ_x is the radial beam size). The system of high-frequency separations includes a controllable amplitude-phase modulator for the generation of a self-tuning sinusoidal signal of 409 kHz and a 200 W power amplifier and resonance circuit connected to two deflecting plates with a length of 130 cm. A few experiments in the 1 x 1 collision mode with the use of the above-mentioned system have been performed. The critical beam current unacceptably drops (at 1.85 GeV from 3 to 0.3 mA) in the absence of any separation of orbits in the parasitic collision point. Figure 8 illustrates the experiment, in which the system of electrostatic separation is completely deactivated, but the high-frequency separation is actuated in the parasitic collision point.



Figure 8. An image of colliding beams on screens of the SR monitors, i.e., a 1.1 mA electron (on the left) and 0.3 mA positron (on the right) beam; the voltage amplitude on the high-frequency separation plates is 6.5 kV ($E = 1.85$ GeV), and two positions of the two-turn orbit are visible.

The electron beam current reaches the range of the operating values in this case, and the collision effects are suppressed. Later, we intend to optimize the mode of colliding beams with high-frequency separation and proceed to comparison of the electron and positron spin frequencies under the new conditions.

GUIDING FIELD STABILIZATION SYSTEM

To increase time stability of the VEPP-4M guiding field, the feedback loop was implemented into the power supply control [21]. The field is measured by a precise NMR magnetometer and the error signal is used to correct the power supply current. With the feedback the field ripples are suppressed in the band of 0-0.1 Hz. The long term non-stability of the field was reduced to 10^{-6} . Fig. 9 shows the NMR magnetometer data with the feedback off and on.

The field values in Oersteds approximately correspond to the beam energy in MeV. With the closed feedback loop, the day-to-day beam energy drift is of an order of 1 keV as it has been. For the frequency range $1 \div 100$ Hz decisive contribution to the instability is made by powerful parts of the main field power supply IST. For these frequencies instabilities are not determined by NMR

feedback and control voltage quality. In this regard, it was proposed to investigate the possibility of suppressing high-frequency ripples with an induction method.

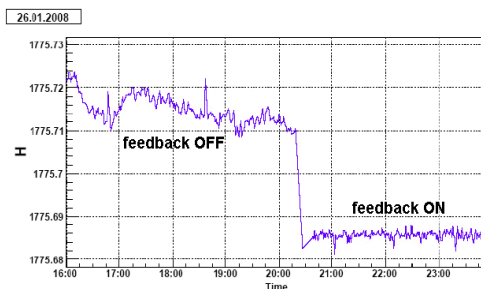


Figure 9: The VEPP-4M guide field stabilization.

The essence of the proposal was measuring the field ripples by the induction sensor to adjust the current in the magnet with the help of parallel connected to IST current generator, which is opposite to the measured ripples. Fig. 10. shows the spectra of the magnetic field fluctuations in terms of $\Delta B / B$, when the broadband compensation is off (upper curve) and on (lower curve). The graph shows that at a frequency of 5 Hz suppression of ripples is more than by 10 times, at a frequency of 10 Hz - 3 times, at a frequency of 30 Hz - 2 times. Attempts to obtain a more effective suppression of magnetic field fluctuations in the band above 50 Hz result in system instability.

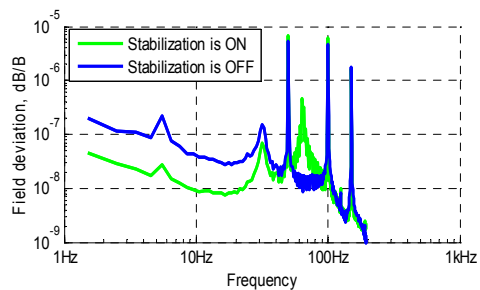


Figure 10: Spectra of magnetic field ripples in the frequencies of 1-100Hz.

In the near future it is planned to achieve the suppression of magnetic ripples in a broad frequency band, as well as to combine the suppression system based on the induction method and the NMR stabilization method. More details of these works are presented in the report [22].

POSSIBILITY OF LUMINOSITY ENHANCEMENT

In early 2014, we performed an experiment in order to increase the luminosity of the collider VEPP_4M at a low energy (< 2 GeV). The radial β -function, β_x , in the collision point has been reduced by two times for this purpose, this has correspondingly increased the monochromatization parameter:

$$\lambda_m = \frac{\sigma_{xs}}{\sigma_{x\beta}} = \frac{\eta_x \sigma_E}{\sqrt{\varepsilon_x \beta_x}}$$

i.e., the ratio of the synchrotron and betatron contributions to the radial beam size, where η_x is the radial dispersion function, σ_E is the relative energy spread, and ε_x is the radial beam emittance. The initial value of this parameter at VEPP-4M is about 2. The physical meaning contained in the λm parameter is most obvious in the limit $\lambda m \rightarrow \infty$, when the betatron contribution to this value is negligibly small. The dependence of the vertical action on the particle from the side of the colliding beam on the horizontal betatron oscillations of the particle itself (x) is eliminated in this case. Thus, the effect of coupling resonances is suppressed. If an increase in the λm value is a finite quantity, then the critical current will increase due to a decrease in the linear radial frequency shift at the collision effects,

$$\xi_x = \frac{Nr_e}{2\pi\gamma} \cdot \frac{\beta_x^*}{\sigma_x^2},$$

and the critical frequency shift by the vertical direction

$$\xi_y = \frac{Nr_e}{2\pi\gamma} \cdot \frac{\beta_y^*}{\sigma_y^* \cdot \sigma_x}$$

will increase due to the suppression of coupling resonances. Numerical simulation [23] of the collision effects shows an increase in the critical current from 3 to 5 mA in the case of reducing the value by two times (Fig. 11). An appreciable luminosity enhancement proportional to the product of the beam current and critical vertical frequency shift is expected.

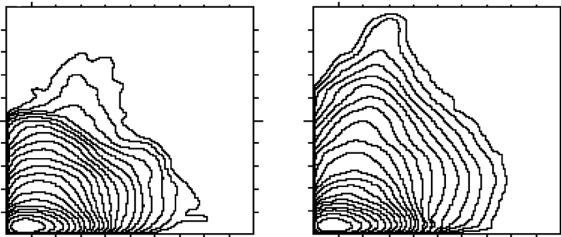


Figure 11. The equilibrium distribution of the normalized betatron amplitudes on a plane in two cases that differ in the values of the beam current, functions, and the resulting parameter ξ_y ($E = 1.85$ GeV). On the left: $I = 3$ mA, $\beta_x = 65$ cm, $\xi_y = 0.036$. On the right: $I = 5$ mA, $\beta_x = 32.5$ cm, $\xi_y = 0.053$.

The experiment, after double decrease of β_x at the interaction point, resulted in increasing of a threshold current (collision effects) by half, accompanied by β_x beating at the ring though. After studying the problem, experiments will be continued.

ACKNOWLEDGMENTS

This work was supported by the Ministry of Education and Science of the Russian Federation and the Russian Foundation for Basic Research (grants nos.10_02_00645, 11_02_01064, 11_02_01422, and 10_02_00904) and the Siberian Branch of the Russian Academy of Sciences (integration grant no. 103).

REFERENCES

- [1] A. Aleshchev, V. Anashin, O. Anchugov, A. Batrakov, E. Behtenev, V. Blinov, A. Bogomyagkov, D. Burenkov, S. Vasichev, S. Glukhov, Yu. Glukhovchenko, O. Gordeev, V. Erokhov, K. Zolotarev, V. Zhilich, A. Zhmaka, A. Zhuravlev*, V. Kaminsky, S. Karnev, G. Karpov, V. Kiselev, G. Kulipanov, E. Kuper, K. Kuper, G. Kurkin, O. Meshkov, S. Mishnev, I. Morozov, N. Muchnoi, V. Neifeld, I. Nikolaev, D. Nikolenko, I. Okunev*, A. Onuchin, A. Pavlenko, V. Petrov, P. Piminov*, O. Plotnikova, A. Poyansky, Yu. Pupkov, V. Sandryev, V. Svistchev, I. Sedliarov, E. Simonov, S. Sinyatkin*, A. Skrinsky, E. Starostina, Yu. Tikhonov, D. Toporkov, K. Todyshev, G. Tumaikin, A. Shamov, D. Shatilov, D. Shvedov, E. Shubin, S. Nikitin.
- * Novosibirsk State Technical University
- [2] V. Anashin et al., BINP Preprint 2011-20, 136 pages.
- [3] V.V. Anashin et al., Physics of particles and nuclei, Vol.44 No.4 (2013) 657-702.
- [4] V.E. Blinov et al., NIM A 494 (2002) 81.
- [5] V.E. Blinov et al. NIM, A598(2009)23.
- [6] O. Anchugov, et al. Instr. Exp. Tech. **53**, no. 1, 15 (2010).
- [7] V.E. Blinov et al. Yader. Fizika 72, N 3, p. 1-6 (2009).
- [8] V. Anashin et al. JETP, 2009, V.109, N4, pp. 590-601
- [9] V.E. Blinov et al. Nuclear Physics B 189(2009)21-23.
- [10] V.E. Blinov et al. Phys. Letters B 686 (2010) 84-90.
- [11] V.E. Blinov et al. Phys. Letters B 685 (2010) 134-140
- [12] V.E. Blinov et al. Phys. Letters B 703 (2011) 543-546.
- [13] V. Anashin et al. Physics Letters B 711(2012)280-291
- [14] V. Anashin et al. Physics Letters B 711(2012)292-300.
- [15] V.M. Aulchenko et al. Phys. Lett. B 731 (2014) 227.
- [16] D.M. Nikolenko et al. Phys. Atom. Nucl. 73 (2010) 1322-1338.
- [17] <http://ssrc.inp.nsk.su/conf/SR2014>
- [19] E. Behtenev et al. Upgrade of BPM system at VEPP-4M collider, these Proceedings.
- [20] V. E. Blinov et al, BINP, Preprint 2013-12, 18 pages
- [21] V.E. Blinov, et al., ICFA Beam Dynamics Newsletters, No. 48, April 2009, pp. 209-217.
- [22] A. Pavlenko et al. Method of Broadband Stabilization of the VEPP-4M Main Field, these Proceedings.
- [23] D. Shatilov, Particle Accelerators 52, 65-93 (1996).